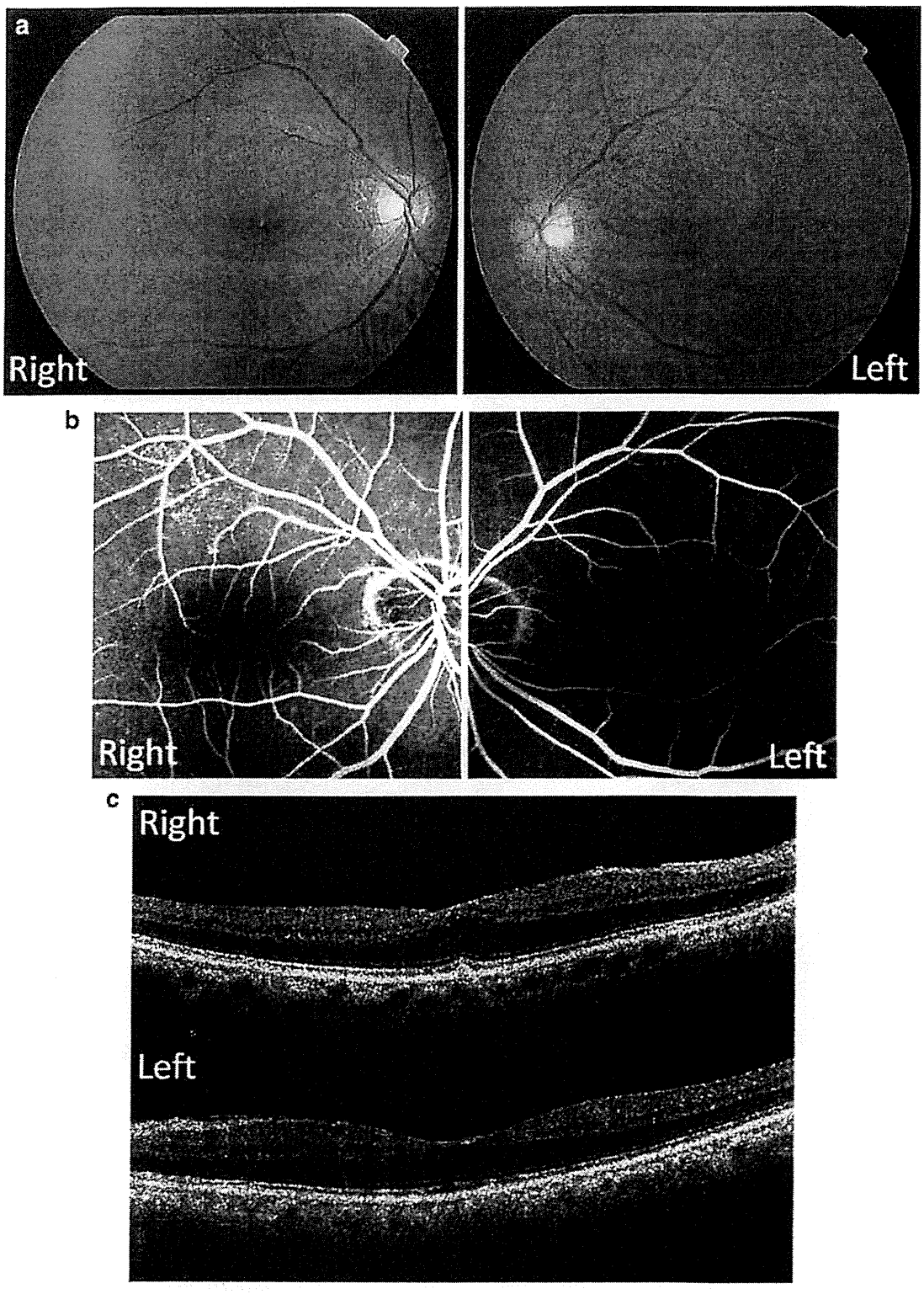


**Fig. 1** Fundus photography, fluorescein angiography, and SD-OCT performed at the initial visit of the patient. **a** Fundus photographs revealed no abnormality in either eye. **b** Fundus fluorescence angiography revealed no abnormality in either eye. **c** Spectral domain-optical coherence tomography (SD-OCT) images for a 6-mm horizontal scan of the retina were essentially normal, with the exception of a slight irregularity of the retinal pigment epithelium in both eyes

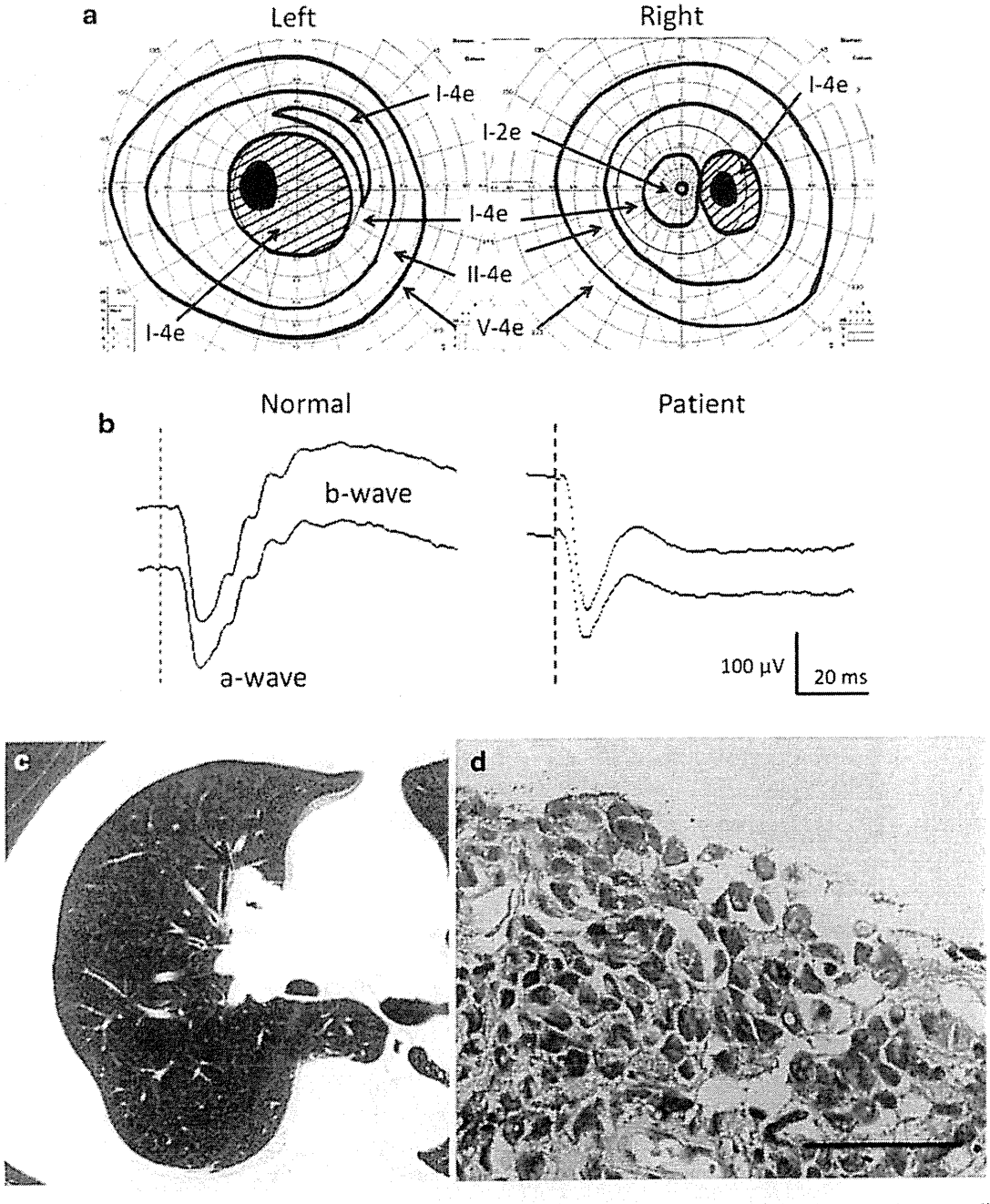


**Fig. 2** Goldmann visual fields, full-field ERGs, CT of the right lung, and histology of a specimen obtained from the hilar lymph node of the patient. **a** Goldmann visual fields revealed a relative central scotoma including the blind spot OD and a relative scotoma around the blind spot OS. **b** Full-field electroretinograms (ERGs) with a bright flash stimulus after dark adaptation showed a "negative-type" pattern for the patient (*right*) compared with the normal pattern (*left*). **c** A computed tomography (CT) scan revealed a tumor in the right lung (*red arrow*). **d** Hematoxylin–eosin staining of a biopsy specimen obtained from a hilar lymph node in the right lung revealed spindle-shaped malignant cells. *Scale bar* 50 µm

TRPM1 is a component of the visual transduction cation channel specifically expressed in retinal ON bipolar cells [15–17, 19]. Immunohistology of the adult mouse retina revealed punctate TRPM1 signals at the tips of ON bipolar cell dendrites detected with antibodies to metabotropic glutamate receptor 6 (mGluR6) and to the α subunit of the $G_o$ protein [16]. TRPM1-null mice were also shown to lack ON bipolar cell responses to light [15, 16]. In addition, *TRPM1* mutations have been associated with the complete form of congenital stationary night blindness (CSNB) in

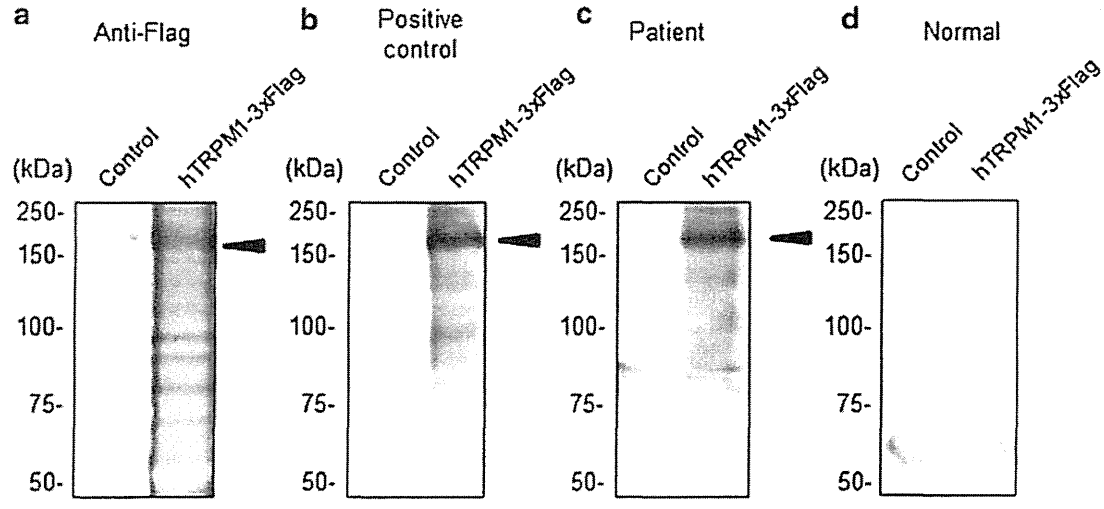


Fig. 3 Immunoblot analysis of serum from the patient for reactivity with TRPM1. HEK293T cells transfected with the expression vector pCAGGS alone (*control*) or with pCAGGS encoding human transient receptor potential cation channel, subfamily M, member 1 (*TRPM1*) tagged with three copies of the flag epitope were subjected to immunoblot analysis with antibodies to the flag tag (**a**), with serum from a patient previously shown to contain autoantibodies to TRPM1 as a positive control (**b**), with serum from the proband (**c**), and with normal control serum (**d**). *Arrowheads* indicate the 3× flag-tagged TRPM1 protein, which showed substantial reactivity with serum from the proband. The positions of molecular size standards (in kilodaltons) are also shown

humans, which is characterized by pronounced dysfunction of the retinal ON pathway [20–23]. These observations suggest that TRPM1 plays a key role in synaptic transmission from photoreceptors to ON bipolar cells. It is possible that ectopic expression of TRPM1 in the malignant melanoma cells of the patient triggered the production of autoantibodies to this protein by B lymphocytes. These antibodies might then have reacted with TRPM1 in retinal ON bipolar cells, resulting in severe dysfunction of the retinal ON pathway.

The average latency from the diagnosis of melanoma to that of MAR was previously found to be 3.6 years, with a range of 2 months–19 years [5]. We diagnosed the present patient with malignant melanoma after only 18 days from the time of his first visit. However, he died 11 months later as a result of metastasis to several organs. In the present case, the visual symptoms preceded the diagnosis of malignant melanoma. The patient complained of blurred vision, night blindness, and photopsia; but Fundus photographs, fluorescein angiograms, and SD-OCT findings were all essentially normal at his initial visit. Perimetry revealed relative scotomas OU. It was his "negative-type" ERGs, indicative of extensive bipolar cell dysfunction, that led us to suspect the patient might have MAR. We, therefore, recommend that ERGs be performed on patients with progressive visual disturbance of unknown origin.

"Negative-type" ERGs are also observed in patients with CSNB. A previous study [5] found that 18 of 27 patients with MAR showed either central or paracentral scotomas or depressions, and 6 of 27 patients had arcuate visual field defects. The present patient had relative central scotomas that included or surrounded the blind spot. In contrast, patients with CSNB manifest a largely intact visual field. MAR patients also show a greater loss of S (blue) cone sensitivity by perimetry than do CSNB patients, and S cone ERGs were not detected in MAR patients [2]. Two subtypes of CAR were previously identified [2]: one in which cone cells are damaged and in which Goldmann perimetry reveals central scotoma, and one in which rod cells are damaged and in which Goldmann perimetry reveals annular scotoma. We speculate that the visual field disturbance of the present patient reflected damage to cone cells.

Drug therapy for MAR is aimed at immunomodulation in order to attenuate the autoimmune attack on the retina before irreversible damage occurs. Treatments include corticosteroid administration, plasmapheresis, intravenous injection of immunoglobulin and immunosuppression. However, the effectiveness of these treatments remains unclear. Oral corticosteroid treatment alone was found to be beneficial in only one of seven patients [5]. In the present study, the patient was treated with oral prednisolone. We believe that this treatment was effective because the vitreous opacity and enlarged blind spots were markedly attenuated after its onset. Further studies are needed to determine the optimal treatment for MAR.

There are several limitations to our study. First, we recorded only bright-flash ERGs after dark adaptation; we did not record rod responses to low-intensity stimuli, photopic responses, or photopic ERGs in response to a

long-duration stimulus in order to determine whether the postreceptor ON pathway was specifically affected. Second, we did not perform immunohistochemical analysis with the serum of the patient to confirm that the autoantibodies recognize retinal bipolar cells. And third, we did not confirm that the autoantibodies actually reacted with malignant melanoma proteins.

In conclusion, we described a Japanese patient with MAR whose serum was positive for autoantibodies to TRPM1. Visual symptoms preceded the identification of malignant melanoma in this patient, and his "negative-type" ERGs led us to suspect a diagnosis of MAR. Further studies are warranted to determine both the proportion of MAR patients who develop TRPM1 autoantibodies as well as the best treatment option for this type of paraneoplastic retinopathy.

**Acknowledgments** We thank Mr. Takahisa Furukawa (Institute for Protein Research, Osaka University) for providing the expression vector for TRPM1 as well as Dr. Duco I. Hamasaki for editing the manuscript.

**Conflicts of interest** Y. Morita, None; K. Kimura, None; Y. Fujitsu, None; A. Enomoto, None; S. Ueno, None; M. Kondo, None; K. Sonoda, None.

## References

1. Berson EL, Lessell S. Paraneoplastic night blindness with malignant melanoma. Am J Ophthalmol. 1988;106:307–11.
2. Milam AH, Saari JC, Jacobson SG, Lubinski WP, Feun LG, Alexander KR. Autoantibodies against retinal bipolar cells in cutaneous melanoma-associated retinopathy. Invest Ophthalmol Vis Sci. 1993;34:91–100.
3. Potter MJ, Thirkill CE, Dam OM, Lee AS, Milam AH. Clinical and immunocytochemical findings in a case of melanoma-associated retinopathy. Ophthalmology. 1999;106:2121–5.
4. Lei B, Bush RA, Milam AH, Sieving PA. Human melanoma-associated retinopathy (MAR) antibodies alter the retinal ON response of the monkey ERG in vivo. Invest Ophthalmol Vis Sci. 2000;41:262–6.
5. Keltner JL, Thirkill CE, Yip PT. Clinical and immunologic characteristics of melanoma-associated retinopathy syndrome: eleven new cases and a review of 51 previously published cases. J Neuroophthalmol. 2001;21:173–87.
6. Alexander KR, Barnes CS, Fishman GA, Milam AH. Nature of the cone ON pathway dysfunction in melanoma-associated retinopathy. Invest Ophthalmol Vis Sci. 2002;43:1189–97.
7. Chan JW. Paraneoplastic retinopathies and optic neuropathies. Surv Ophthalmol. 2003;48:12–38.
8. Adamus G. Autoantibody targets and their cancer relationship in the pathogenicity of paraneoplastic retinopathy. Autoimmun Rev. 2009;8:410–4.
9. Potter MJ, Adamus G, Szabo SM, Lee R, Mohaseb K, Behn D. Autoantibodies to transducin in a patient with melanoma-associated retinopathy. Am J Ophthalmol. 2002;134:128–30.
10. Hartmann TB, Bazhin AV, Schadendorf D, Eichmuller SB. SEREX identification of new tumor antigens linked to melanoma-associated retinopathy. Int J Cancer. 2005;114:88–93.
11. Lu Y, Jia L, He S, Hurley MC, Leys MJ, Jayasundera T, et al. Melanoma-associated retinopathy: a paraneoplastic autoimmune complication. Arch Ophthalmol. 2009;127:1572–80.
12. Bazhin AV, Dalke C, Willner N, Abschütz O, Wildberger HGH, Philippov PP, et al. Cancer-retina antigens as potential paraneoplastic antigens in melanoma-associated retinopathy. Int J Cancer. 2009;124:140–9.
13. Dhingra A, Fina ME, Neinstein A, Ramsey DJ, Xu Y, Fishman GA, et al. Autoantibodies in melanoma-associated retinopathy target TRPM1 cation channels of retinal ON bipolar cells. J Neurosci. 2011;31:3962–7.
14. Kondo M, Sanuki R, Ueno S, Nishizawa Y, Hashimoto N, Ohguro H, et al. Identification of autoantibodies against TRPM1 in patients with paraneoplastic retinopathy associated with ON bipolar cell dysfunction. PLoS One. 2011;6:e19911.
15. Morgans CW, Zhang J, Jeffrey BG, Nelson SM, Burke NS, Duvoisin RM, et al. TRPM1 is required for the depolarizing light response in retinal ON bipolar cells. Proc Natl Acad Sci USA. 2009;106:19174–8.
16. Koike C, Obara T, Uriu Y, Numata T, Sanuki R, Miyata K, et al. TRPM1 is a component of the retinal ON bipolar cell transduction channel in the mGluR6 cascade. Proc Natl Acad Sci USA. 2010;107:332–7.
17. Koike C, Numata T, Ueda H, Mori Y, Furukawa T. TRPM1: a vertebrate TRP channel responsible for retinal ON bipolar function. Cell Calcium. 2010;48:95–101.
18. Loduca AL, Zhang C, Zelkha R, Shahidi M. Thickness mapping of retinal layers by spectral-domain optical coherence tomography. Am J Ophthalmol. 2010;150:849–55.
19. Klooster J, Blokker J, Ten Brink JB, Unmehopa U, Fluiter K, Bergen AA. Ultrastructural localization and expression of TRPM1 in the human retina. Invest Ophthalmol Vis Sci. 2011;52:8356–62.
20. Li Z, Sergouniotis PI, Michaelides M, Mackay DS, Wright GA, Devery S, et al. Recessive mutations of the gene TRPM1 abrogate ON bipolar cell function and cause complete congenital stationary night blindness in humans. Am J Hum Genet. 2009;85:711–9.
21. van Genderen MM, Bijveld MM, Claassen YB, Florijn RJ, Pearring JN, Meire FM, et al. Mutations in TRPM1 are a common cause of complete congenital stationary night blindness. Am J Hum Genet. 2009;85:730–6.
22. Audo I, Kohl S, Leroy BP, Munier FL, Guillonneau X, Mohand-Saïd S, et al. TRPM1 is mutated in patients with autosomal-recessive complete congenital stationary night blindness. Am J Hum Genet. 2009;85:720–9.
23. Nakamura M, Sanuki R, Yasuma TR, Onishi A, Nishiguchi KM, Koike C, et al. TRPM1 mutations are associated with the complete form of congenital stationary night blindness. Mol Vis. 2010;16:425–37.

Clinical Ophthalmology

Dove

CASE REPORT

# Peripheral capillary nonperfusion and full-field electroretinographic changes in eyes with frosted branch-like appearance retinal vasculitis

Yoshitsugu Matsui
Hideyuki Tsukitome
Eriko Uchiyama
Yuko Wada
Tatsuya Yagi
Hisashi Matsubara
Mineo Kondo

Department of Ophthalmology, Mie University Graduate School of Medicine, Tsu, Japan

**Abstract:** We report a patient with frosted branch-like appearance retinal vasculitis associated with peripheral capillary nonperfusion and full-field electroretinographic changes. A 62-year-old man presented with sudden bilateral decreased vision accompanied by headaches. His best-corrected visual acuity was 0.01 in both eyes. Fundus examination and fluorescein angiography showed bilateral frosted branch-like appearance retinal vasculitis, and spectral-domain optical coherence tomography showed severe macular edema in both eyes. The cerebrospinal fluid analyses showed an increased lymphocyte count and protein levels. He was treated with systemic corticosteroid therapy, and his best-corrected visual acuity improved to 0.8 OD and 1.0 OS at 6 months after onset. However, fluorescein angiography showed a lack of capillary perfusion in the periphery, and the oscillatory potentials on full-field electroretinography were severely reduced in both eyes. These findings indicated extensive retinal ischemia and inner retinal dysfunction, and that fluorescein angiography and full-field electroretinograms can be useful during follow-up of eyes with frosted branch-like appearance retinal vasculitis.

**Keywords:** frosted branch angiitis, aseptic meningitis, optical coherence tomography, electroretinogram, oscillatory potentials

## Introduction

Frosted branch angiitis[1] is a rare type of periphlebitis characterized by white sheathing of the retinal vessels in association with different types of inflammatory eye disease.[2–4] The onset of frosted branch angiitis is usually sudden, and patients may complain of painless blurred vision, a central blind area, floaters, and photopsias.

Most patients with frosted branch angiitis respond to systemic corticosteroid therapy with good recovery of visual acuity, but various adverse complications have also been reported. These complications include macular scarring, retinal vein or artery occlusion, macular epiretinal membrane formation, diffuse retinal fibrosis, optic disc atrophy, peripheral capillary nonperfusion, and vitreous hemorrhage, all of which have been reviewed elsewhere.[3]

We report our findings in a 62-year-old man with bilateral frosted branch-like appearance retinal vasculitis accompanied by aseptic meningitis. He was treated with systemic corticosteroid therapy with good recovery of visual acuity. However, examinations at 6 months after onset revealed peripheral capillary nonperfusion and severe reduction of the amplitudes of oscillatory potentials on the electroretinogram. These changes suggested extensive retinal ischemia and inner retinal dysfunction, which required photocoagulation.

Correspondence: Mineo Kondo
Department of Ophthalmology, Mie University Graduate School of Medicine, 2-175 Edobashi, Tsu, 514-8507, Japan
Tel +815 9231 5027
Fax +815 9231 3036
Email mineo@clin.medic.mie-u.ac.jp

## Case report

A 62-year-old man presented with sudden bilateral decrease of vision accompanied by headaches. He did not have any systemic diseases, and his family history revealed no other members with eye disease. He had never experienced oral ulcers or skin lesions previously.

At our initial examination, his best-corrected visual acuity was 0.01 in both eyes, and Goldmann perimetry showed a severe central scotoma in both eyes. The intraocular pressure was 18 mmHg OD and 16 mmHg OS. Slit-lamp examination showed many fine keratic precipitates and cells in the aqueous and vitreous of both eyes. Severe sheathing of the retinal vessels and retinal hemorrhages was detected in both eyes by ophthalmoscopy (Figure 1, upper panel). Fluorescein angiography showed perivenous staining and leakage from the vessels (Figure 1, lower panel). Spectral-domain optical coherence tomography (Spectralis®, Heidelberg Engineering, Heidelberg, Germany) demonstrated severe macular edema with central macular thickness of 1045 μm OD and 991 μm OS (Figure 2, uppermost panel). We also recorded full-field electroretinograms and found that the amplitudes of the mixed rod and cone responses after dark adaptation were severely attenuated in both eyes (Figure 3, middle panel).

On systemic examination, blood count, biochemical analysis including kidney function tests, urine testing, and chest x-rays were within normal limits. Angiotensin-converting enzyme levels were also within normal limits. Tests for syphilis and human immunodeficiency virus were negative.

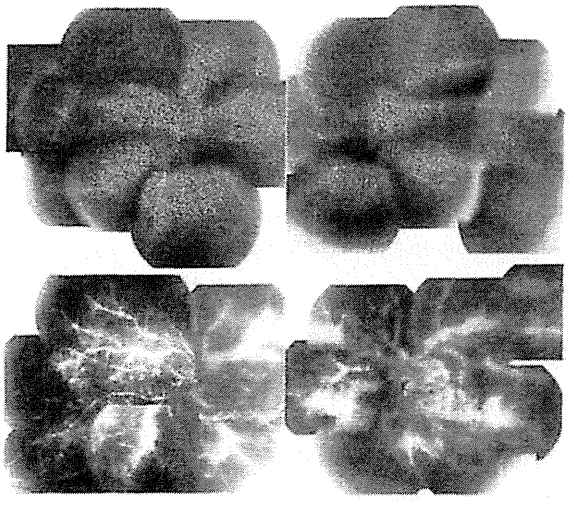

**Figure 1** Fundus photographs and fluorescein angiograms at initial examination showing bilateral diffuse perivascular sheathing and retinal edema with intraretinal hemorrhages (upper panel).
**Note:** Fluorescein angiography shows extensive vascular leakage and retinal edema (lower panel).

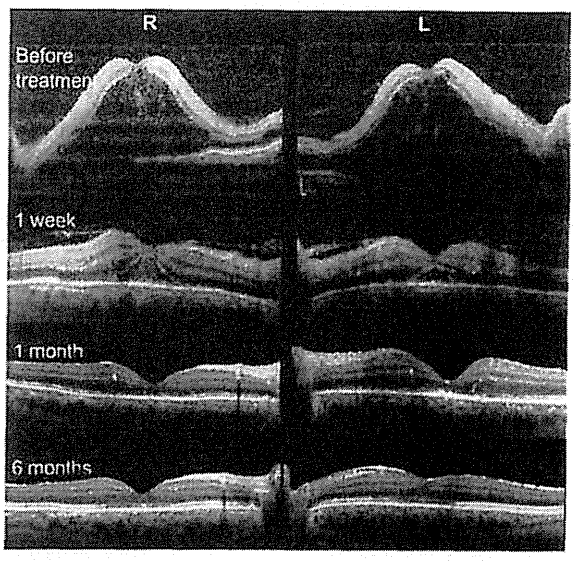


**Figure 2** Changes in spectral-domain optical coherence tomograms at onset, and at one week, one month, and 6 months after treatment.

Lupus anticoagulant and anticardiolipin antibody were not detected. The HLA type was A11, A24, B39, B54, DR4, and DR8. Herpes simplex and varicella zoster IgG antibody titers suggested prior exposure only. Polymerase chain reaction analysis of the aqueous humor was negative for herpes simplex, herpes zoster, and cytomegalovirus DNA. Cerebrospinal fluid analysis disclosed an increased leukocyte count (72/mL, mononuclear cells) and protein level (49 mg/dL; normal 10–40 mg/dL). Cerebrospinal fluid cultures were negative.

Based on the results of these systemic examinations, we diagnosed our patient as having frosted branch-like appearance retinal vasculitis associated with aseptic meningitis. He was treated with pulsed steroid therapy (methylprednisolone 1000 mg/day × 3 days) followed by oral prednisolone (1 mg/kg/day), topical steroids, and mydriasis.

One month later, the patient's best-corrected visual acuity improved to 0.6 (OD) and 0.5 (OS), and spectral-domain optical coherence tomography showed a reduction in macular edema (Figure 2, third panel).

Six months after the start of steroid therapy, best-corrected visual acuity was improved to 0.8 OD and 1.0 OS and the fundus had returned to nearly normal (Figure 4, upper panel). Spectral-domain optical coherence tomography showed that the thickness of the retina was normal but the inner segment/outer segment junction of the photoreceptors was still disrupted at the fovea in both eyes (Figure 2, lowest panel). We performed fluorescein angiography again, and found that there were extensive areas without capillary perfusion in the

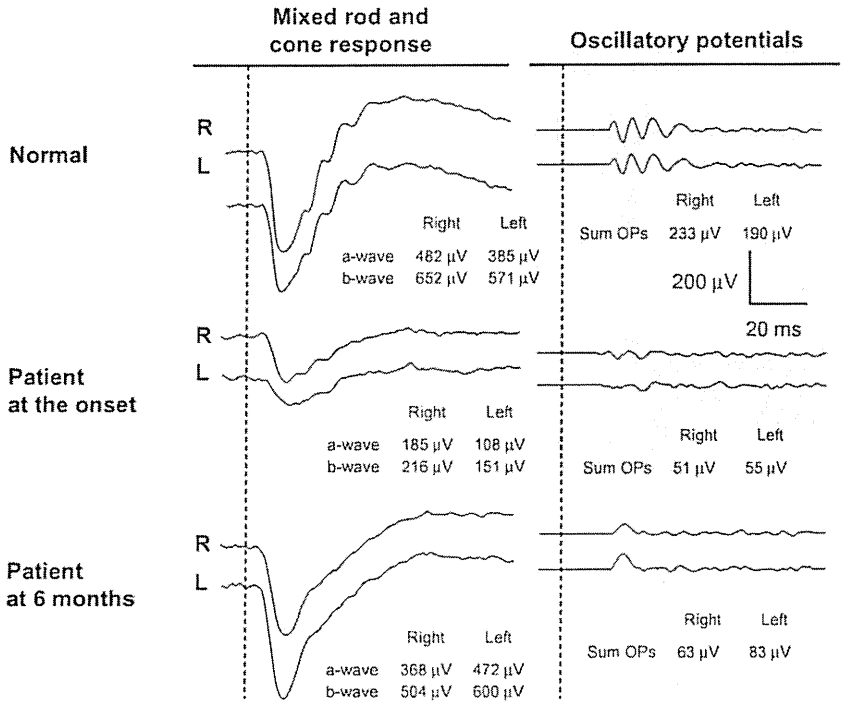


**Figure 3** Changes in full-field electroretinograms.
**Notes:** Full-field mixed rod and cone electroretinograms were recorded after 20 minutes of dark adaptation at onset and 6 months after treatment. Full-field electroretinograms were elicited by a contact lens electrode with a built-in white light emitting diode (LE-2000, Tomey Co, Nagoya, Japan).[11] The stimulus intensity was 10.0 cd-s/m$^2$ (photopic units). Although the a-waves and b-waves recovered to normal, the oscillatory potentials were still severely reduced at 6 months after onset.

periphery of both eyes (Figure 4, lower panel). Full-field electroretinograms demonstrated nearly normal a waves and b waves, but severely reduced oscillatory potentials in both eyes (Figure 3, lowest panel). These results suggested extensive retinal ischemia and inner retinal dysfunction.

We then performed photocoagulation of the peripheral retina to prevent neovascularization and vitreous hemorrhage. There were no retinal complications in our patient during one year of follow-up after photocoagulation.

## Discussion

Frosted branch angiitis is considered to be a clinical subtype of diffuse retinal periphlebitis and is associated with various types of systemic and ocular disease.[2–4] Frosted branch angiitis is reported to be associated with virus and bacterial infections, lymphoma, leukemia, Crohn's disease, systemic lupus, toxoplasmosis, Behçet's disease, central retinal vein occlusion, nephritis, and other systemic diseases.[2–4] The frosted branch-like appearance retinal vasculitis in our patient was believed to be associated with aseptic meningitis because he had headaches and an increased lymphocyte count and protein level in his cerebrospinal fluid. Further, no viral infection could be detected.

Johkura et al[5] reported a 20-year-old woman with frosted branch angiitis and aseptic meningitis who had headaches, nausea, and vomiting, and cerebrospinal fluid study showed lymphocyte counts increased to 83/mL and a protein level of 42 mg/dL. More recently, Chaume et al[6] reported an 11-year-old boy with frosted branch angiitis and aseptic meningitis. Their clinical findings and laboratory data were very similar to those in our patient.

In our patient, fluorescein angiography showed extensive areas without capillary perfusion in the peripheral retina and a selective reduction in amplitudes of the oscillatory potentials in both eyes. It is widely accepted that oscillatory potentials originate mainly from inhibitory neural pathways in the inner retina, including those of the amacrine and ganglion cells.[7] It has also been reported that a selective reduction in the amplitude of oscillatory potentials is also found when inner retinal function is extensively impaired, eg, in diabetic retinopathy or central retinal vein occlusion.[7] Thus, the findings of a lack of peripheral capillary perfusion and selective loss of oscillatory potentials on the electroretinogram in our patient strongly suggest that the retina was extensively ischemic and required photocoagulation. Luo et al[8] also used full-field electroretinograms during follow-up of a

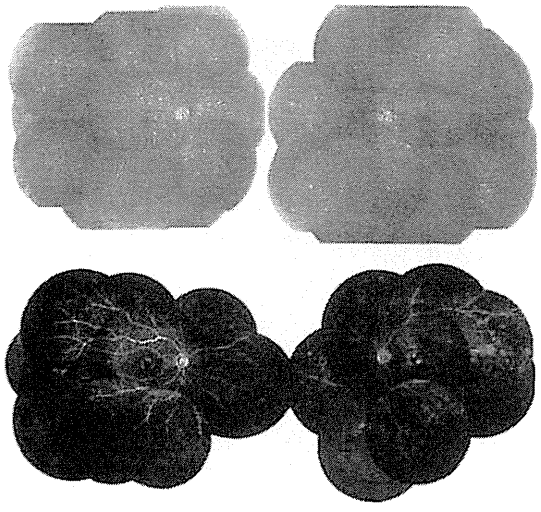

**Figure 4** Fundus photographs and fluorescein angiograms 6 months after treatment.
**Note:** The fundus had recovered to nearly normal, but the fluorescein angiograms show extensive lack of capillary perfusion in the peripheral retina (lower panel).

5-year-boy with frosted branch angiitis, but reported that all electroretinographic components recovered to normal 6 months after treatment.

Our search using PubMed and the Japan Medical Abstracts Society yielded only three papers on frosted branch angiitis associated with peripheral capillary nonperfusion. In 1988, Kleiner et al[2] reported a 25-year-old man with frosted branch angiitis who developed multiple branch vein occlusion, capillary nonperfusion, and retinal neovascularization. In 1989, Terasaki et al[9] reported on a 21-year-old woman with frosted branch angiitis, who developed peripheral capillary nonperfusion and retinal neovascularization which required panretinal photocoagulation 18 months after onset. In 1993, Harigai et al[10] reported on a 39-year-old man with frosted branch angiitis who developed peripheral capillary nonperfusion at 7 months after onset. Despite panretinal photocoagulation, vitreous hemorrhages developed in his right eye. Although fluorescein angiography was repeatedly performed during follow-up, full-field electroretinograms were not recorded in these three patients.

The findings in our case suggest that extensive retinal ischemia and inner retinal dysfunction can occur in eyes with frosted branch-like appearance retinal vasculitis, and careful follow-up examinations are needed, even after good recovery of visual acuity. In addition to fluorescein angiography, full-field electroretinography may be useful during follow-up of these patients.

## Acknowledgments

Funding for this work was received from the Ministry of Education, Culture, Science and Technology (23592603), Japan. The authors thank Duco I Hamasaki for editing the manuscript.

## Disclosure

The authors report that they have no competing interests in this work.

## References

1. Ito Y, Nakano M, Kyu N, Takeuchi M. Frosted branch angiitis in a child. *Rinsho Ganka*. 1976;30(7):797–803. Japanese.
2. Kleiner RC, Kaplan HJ, Shakin JL, Yannuzzi LA, Crosswell HH Jr, McLean WC Jr. Acute frosted retinal periphlebitis. *Am J Ophthalmol*. 1998;106(1):27–34.
3. Walker S, Iguchi A, Jones NP. Frosted branch angiitis: a review. *Eye (Lond)*. 2004;18(5):527–533.
4. Kleiner RC. Frosted branch angiitis: clinical syndrome or clinical sign? *Retina*. 1997;17(5):370–371.
5. Johkura K, Hara A, Hattori T, Hasegawa O, Kuroiwa Y. Frosted branch angitis associated with aseptic meningitis. *Eur J Neurol*. 2000;7(2):241.
6. Chaume A, Lemelle I, Chastagner P, Angioi K. A case report of frosted branch angiitis associated with aseptic meningitis in a young boy. *J Fr Ophtalmol*. 2011;34(2):129. e1–e5. French.
7. Wachtmeister L. Oscillatory potentials in the retina: what do they reveal. *Prog Retin Eye Res*. 1998;17(4):485–521.
8. Luo G, Yang P, Huang S, Jiang F, Wen F. A case report of frosted branch angiitis and its visual electrophysiology. *Doc Ophthalmol*. 1998–1999;97(2):135–142.
9. Terasaki H, Yanagida K, Tanaka T. An adult case of frosted branch angiitis with various systemic manifestation. *Folia Ophthalmol Jpn*. 1989;40(11):2438–2442. Japanese.
10. Harigai R, Seki R, Emi K, Oguro Y, Sato Y. A case of frosted branch angiitis associated with vitreous hemorrhage. *Folia Ophthalmol Jpn*. 1993;44(6):772–778. Japanese.
11. Kondo M, Piao CH, Tanikawa A, Horiguchi M, Miyake Y. A contact lens electrode with built-in high intensity white light-emitting diodes. *Doc Ophthalmol*. 2001;102(1):1–9.

Jpn J Ophthalmol (2014) 58:232–236
DOI 10.1007/s10384-014-0316-6

THE OFFICIAL INTERNATIONAL JOURNAL OF THE JAPANESE OPHTHALMOLOGICAL SOCIETY

CLINICAL INVESTIGATION

# Electroretinograms and level of aqueous vascular endothelial growth factor in eyes with hemicentral retinal vein occlusion or branch retinal vein occlusion

**Shunsuke Yasuda · Shu Kachi · Shinji Ueno · Hiroaki Ushida · Chang-Hua Piao · Mineo Kondo · Hiroko Terasaki**

Received: 14 August 2013 / Accepted: 14 February 2014 / Published online: 26 March 2014


**Abstract**
*Purpose* Hemicentral retinal vein occlusion (hCRVO) is a disease related to CRVO but not to branch retinal vein occlusion (BRVO). We reported a significant correlation between aqueous vascular endothelial growth factor (VEGF) levels and the implicit time of 30-Hz flicker electroretinogram (ERG) in CRVO eyes. The purpose of this study was to compare aqueous VEGF levels and ERG components between hCRVO and BRVO eyes.
*Methods* The medical records of patients with macular edema secondary to hCRVO (12 eyes) or BRVO (16 eyes) and received an intravitreal injection of bevacizumab (IVB) at the Nagoya University Hospital from July 2009 to May 2013 were reviewed. Full-field ERGs were recorded before the IVB. Aqueous humor was collected just before the IVB to measure VEGF concentration. Differences in aqueous VEGF level and ERG components between hCRVO and BRVO eyes were determined.
*Results* Mean aqueous VEGF concentration in hCRVO eyes was significantly higher than that in BRVO eyes (504 vs. 148 pg/ml, $P < 0.05$). The implicit time of 30-Hz flicker ERG was significantly longer in hCRVO than in BRVO eyes (33.5 vs. 29.8 ms, $P < 0.01$).
*Conclusion* The significant difference in VEGF levels in aqueous and implicit times of 30-Hz flicker ERG suggest that retinal ischemia is more manifest in hCRVO than in BRVO eyes.

S. Yasuda · S. Kachi (✉) · S. Ueno · H. Ushida · C.-H. Piao · M. Kondo · H. Terasaki
Department of Ophthalmology, Nagoya University Graduate School of Medicine, 65 Tsuruma-cho, Showa-ku, Nagoya 466-8550, Japan
e-mail: kachishu-ngy@umin.ac.jp

**Keywords** Hemicentral retinal vein occlusion · Branch retinal vein occlusion · Electroretinogram · Vascular endothelial growth factor

## Introduction

Hemicentral retinal vein occlusion (hCRVO) is a disease related to CRVO but not to branch retinal vein occlusion (BRVO). It is reported that in a certain proportion of human eyes, a two-trunked central retinal vein (CRV) may persist in the anterior part of the optic nerve as a congenital anomaly. One of the two trunks may be occluded in the optic nerve to produce hCRVO. On the other hand, BRVO typically occurs at an arteriovenous crossing [1, 2]. CRVO instigates retinal ischemia, which induces up-regulation of vascular endothelial growth factor (VEGF), which leads to iris neovascularization [3–7]. Similar changes occur in eyes with hCRVO but not in eyes with BRVO. It is reported that VEGF levels in the vitreous were significantly higher in eyes with CRVO and hCRVO than in eyes with BRVO [8]. Results of several studies demonstrate that different components of full-field electroretinograms (ERGs) can be helpful in distinguishing ischemic from nonischemic CRVO [9–26]. We showed that implicit times of 30-Hz flicker ERG were significantly correlated with ocular VEGF level in CRVO eyes [27], and Noma et al. [28] report that they were significantly correlated with ocular VEGF level in BRVO eyes. However, little is known about the comparison of ERG parameters and ocular VEGF concentrations between hCRVO and BRVO eyes. The purpose of this study was to determine whether there are any differences in VEGF levels in the aqueous and in amplitudes and implicit times of different ERG components between hCRVO and BRVO eyes.

## Patients and methods

The procedures used in this study conformed to the tenets of the World Medical Association's Declaration of Helsinki. The intravitreal injection of bevacizumab (IVB), collection of aqueous humor, and VEGF measurements were performed after obtaining approval of Nagoya University Hospital Ethics Review Board and a written informed consent from each patient.

### Patients

We reviewed medical records of patients with macular edema secondary to hCRVO or BRVO and who received an IVB at the Nagoya University Hospital from July 2009 to May 2013. Patients with diabetic retinopathy were excluded.

### Electroretinograms

Full-field ERGs, elicited by stimuli from a Ganzfeld dome, were recorded before IVB with a Burian–Allen bipolar contact lens electrode. The eyes were dark adapted for 30 min, and a rod response was elicited by blue light at an intensity of $5.2 \times 10^3$ cd/s/m$^2$. A mixed cone–rod ERG was elicited by a white flash of 44.2 cd/s/m$^2$, and cone ERGs and 30-Hz flicker ERGs were elicited by white stimuli of 4 and 0.9 cd/s/m$^2$, respectively. Cone and flicker ERGs were elicited by stimuli on a white background of 68 cd/m$^2$ [27].

### Intravitreal injection of bevacizumab and collection of aqueous humor

The eyes were anesthetized with topical 1 % tetracaine, and the fornices were irrigated with 10 % povidone–iodine. A mean volume of 0.1 ml of aqueous humor was collected by anterior-chamber paracentesis with a 27-gauge needle attached to a 1-ml syringe. Each patient then received an intravitreal injection of 1.25 mg/0.05 ml bevacizumab using a 30-gauge needle inserted through the sclera 3.5 mm from the limbus. Antibiotics drops were given for 3 days after the injection [27].

### Measurement of VEGF level in aqueous by ELISA

Aqueous samples were stored at −80 °C until use. VEGF concentration was measured using enzyme-linked immunosorbent assay (ELISA) using a commercially available kit (Quantikine; R&D Systems, Minneapolis, MN, USA), which measures human VEGF121 and VEGF165 [27].

### Statistical analyses

The significance of differences in VEGF levels of aqueous humor and ERG parameters between hCRVO and BRVO eyes was determined with the Mann–Whitney $U$ test. Commercially available software (SPSS v. 17.0J for Windows; SPSS Inc., Chicago, IL, USA) was used for all statistical analyses. $P < 0.05$ was considered significant.

## Results

### Patients

Demographics of the patients with hCRVO and BRVO are shown in Table 1. Twenty-eight eyes of 28 patients with macular edema secondary to hCRVO ($n = 12$) and BRVO ($n = 16$) were studied. There were nine men and three women in the hCRVO group and nine men and seven women in the BRVO group. Mean age was 66.9 years in the hCRVO group and 61.6 years in the BRVO group. Mean visual acuity before IVB was 0.69 logarithm of the minimum angle of resolution (logMAR) units in the hCRVO group and 0.45 logMAR units in the BRVO group. Mean duration of symptoms before IVB was 15.6 weeks in the hCRVO group and 14.3 weeks in the BRVO group.

Fluorescein angiography showed that eight patients with hCRVO and four with BRVO had a nonperfusion area (NPA), although none of the NPA was >10 DA (disc area) in size. Photocoagulation was applied to the NPA of these patients after IVB. There was no angle or iris neovascularization in any patient.

### Comparison of ERG components between hCRVO and BRVO eyes

Rod, cone, single bright flash, and 30-Hz flicker ERG amplitudes of hCRVO group and BRVO group eyes are shown in Table 2; implicit times of the same parameters are shown in Table 3. Implicit times of 30-Hz flicker ERG of hCRVO eyes were significantly longer than that of BRVO eyes (33.5 ± 3.5 vs. 29.8 ± 2.0 ms; $P = 0.006$). There were no significant differences in the other ERG components.

**Table 1** Characteristics of 28 patients with hemicentral retinal vein occlusion (hCRVO) and branch retinal vein occlusion (BRVO)

| | hCRVO | BRVO | $P$ value |
|---|---|---|---|
| Eyes | 12 | 16 | |
| Age[a] | 66.9 ± 6.4 | 61.6 ± 9.8 | 0.12* |
| Sex (men/women) | 9/3 | 9/7 | 0.31** |
| Visual acuity (logMAR)[a] | 0.69 ± 0.49 | 0.45 ± 0.27 | 0.25* |
| Duration before treatment (weeks)[a] | 15.6 ± 4.1 | 14.3 ± 5.1 | 0.68* |

* Mann–Whitney $U$ test, ** $\chi^2$ test

[a] Data are the means ± standard deviation

**Table 2** Comparison of amplitudes of ERGs between hemicentral retinal vein occlusion (hCRVO) and branch retinal vein occlusion (BRVO) eyes

| ERG components | hCRVO eyes (average ± SD) μV[a] | BRVO eyes (average ± SD) μV[a] | *P* value* | Normal control eyes (average ± SD) μV[a] |
|---|---|---|---|---|
| Rod b-wave | 73.5 ± 44.5 | 74.0 ± 24.7 | 0.88 | 101 ± 37.7 |
| Single flash a-wave | 294 ± 75.4 | 298 ± 97.6 | 0.96 | 383 ± 87.4 |
| Single flash b-wave | 419 ± 103 | 400 ± 108 | 0.50 | 535 ± 123 |
| Single flash b/a ratio | 1.37 ± 0.32 | 1.46 ± 0.22 | 0.40 | 1.40 ± 0.19 |
| Cone a-wave | 22.0 ± 5.5 | 28.3 ± 9.5 | 0.09 | 38.0 ± 11.9 |
| Cone b-wave | 58.7 ± 22.6 | 72.1 ± 26.5 | 0.05 | 94.6 ± 42.2 |
| 30-Hz flicker | 22.0 ± 8.6 | 25.9 ± 16.1 | 0.69 | 28.1 ± 12.1 |

*SD* standard deviation

* Mann–Whitney *U* test

[a] Except for the single-flash b/a ratio

**Table 3** Comparison of implicit times of ERGs between hemicentral retinal vein occlusion (hCRVO) and branch retinal vein occlusion (BRVO) eyes

| ERG components | hCRVO eyes (average ± SD) ms | BRVO eyes (average ± SD) ms | *P* value* | Normal control eyes (average ± SD) ms |
|---|---|---|---|---|
| Single flash a-wave | 13.9 ± 1.8 | 13.1 ± 0.7 | 0.23 | 12.6 ± 1.0 |
| Single flash b-wave | 55.6 ± 3.0 | 53.2 ± 3.4 | 0.06 | 52.0 ± 3.1 |
| Cone a-wave | 17.3 ± 2.2 | 16.5 ± 0.9 | 0.47 | 16.2 ± 0.77 |
| Cone b-wave | 33.8 ± 2.6 | 31.8 ± 1.9 | 0.06 | 30.3 ± 1.42 |
| 30-Hz flicker | 33.5 ± 3.5 | 29.8 ± 2.0 | 0.006 | 28.8 ± 2.1 |

*SD* standard deviation

* Mann–Whitney *U* test

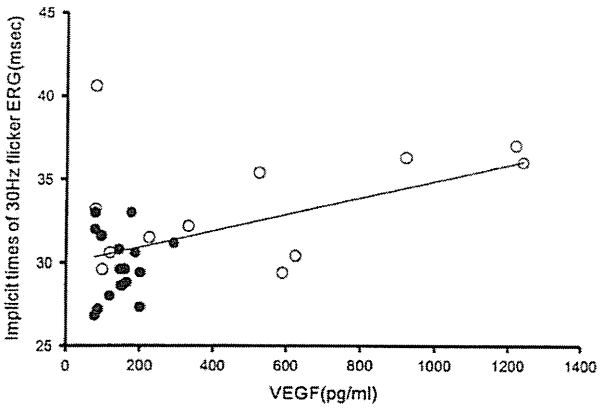


**Fig. 1** Relationship between implicit times of 30-Hz flicker electroretinograms (ERGs) and aqueous vascular endothelial growth factor (VEGF) concentration in all 28 eyes. *Shaded circles* indicate branch retinal vein occlusion (BRVO) eyes, and *circles* indicate hemicentral retinal vein occlusion (hCRVO) eyes

### Comparison of aqueous VEGF concentrations between hCRVO and BRVO eyes

Before the IVB, the mean aqueous VEGF concentration in hCRVO eyes was significantly higher than that in BRVO eyes (504 ± 429 vs. 148 ± 58 pg/ml, $P = 0.04$).

### Relationship between implicit time of 30-Hz flicker ERGs and VEGF concentration in aqueous humor

Coefficients of correlation between the implicit time of the 30-Hz flicker ERGs and the VEGF concentration in aqueous humor were determined by Pearson product-moment correlation coefficient. The implicit times of 30-Hz flicker ERG were significantly correlated with the VEGF concentration in the aqueous in all 28 eyes ($P = 0.01$; $r = 0.50$). However, a significant correlation was not obtained when analysis was performed separately, either on BRVO eyes or hCRVO eyes (Fig. 1).

## Discussion

Our results show that aqueous VEGF concentration was higher and the implicit time of 30-Hz flicker ERG was longer in hCRVO than in BRVO eyes. VEGF level in aqueous humor was consistent with that in the vitreous, as reported by Koss et al. [8]. Those authors found that mean VEGF concentrations in the vitreous were 162 pg/ml in BRVO eyes, 278 pg/ml in hCRVO eyes, and 212 pg/ml in CRVO eyes. Our results show that mean VEGF concentration in aqueous humor was 148 pg/ml in BRVO eyes and 504 pg/ml in hCRVO eyes. In addition, we previously

reported that mean aqueous VEGF concentrations in 20 CRVO eyes was 412 pg/ml, although some eyes were treated by laser before sample collection in that study [27]. Aqueous VEGF concentrations in hCRVO eyes were significantly higher than in BRVO eyes but not lower than in CRVO eyes. The difference in VEGF concentration between findings by Koss et al. and our results may be due to sample differences or the ELISA kit used, as our kit recognizes both VEGF165 and VEGF121. Our earlier study on CRVO eyes shows that the mean implicit time of 30-Hz flicker ERG was 34.3 ms [27]. In our present study, the implicit time of 30-Hz flicker ERG in hCRVO was longer than that in BRVO eyes and similar to that in CRVO eyes. Kjeka et al. [29] report that eyes with CRVO and with 30-Hz flicker ERG >35 ms developed neovascularization. In our study, all eyes with 30-Hz flicker ERG implicit time of >35 ms were hCRVO eyes. Our results appear to be consistent with the fact that hCRVO is a disease unrelated to BRVO and tends to have a higher risk of neovascularization [1, 2]. In conclusion, the significant differences in aqueous VEGF levels and in implicit times of 30-Hz flicker ERG suggest that retinal ischemia is more manifest in hCRVO eyes than in BRVO eyes.

**Acknowledgments** Aichi D.R.G foundation (SK) and Grant-in Aid 23592563 (SK), 25462709 (SU), 23592603 (MK), and 23390401 (HT) from the Ministry of Education, Science, Sports and Culture, Japan. The authors thank Professor Duco Hamasaki of Bascom Palmer Eye Institute for discussions and editing the final version of the manuscript.

**Conflicts of interest** S. Yasuda, None; S. Kachi, None; S. Ueno, None; H. Ushida, None; C.-H. Piao, None; M. Kondo, None; H. Terasaki, None.

## References

1. Hayreh SS, Hayreh MS. Hemicentral retinal vein occulsion. Pathogenesis, clinical features, and natural history. Arch Ophthalmol. 1980;98:1600–9.
2. Hayreh SS. Prevalent misconceptions about acute retinal vascular occlusive disorders. Prog Retin Eye Res. 2005;24:493–519.
3. Aiello LP, Avery RL, Arrigg PG, Keyt BA, Jampel HD, Shah ST, et al. Vascular endothelial growth factor in ocular fluid of patients with diabetic retinopathy and other retinal disorders. N Engl J Med. 1994;331:1480–7.
4. Pe'er J, Folberg R, Itin A, Gnessin H, Hemo I, Keshet E. Vascular endothelial growth factor upregulation in human central retinal vein occlusion. Ophthalmology. 1998;105:412–6.
5. Tripathi RC, Li J, Tripathi BJ, Chalam KV, Adamis AP. Increased level of vascular endothelial growth factor in aqueous humor of patients with neovascular glaucoma. Ophthalmology. 1998;105:232–7.
6. Suzuki Y, Nakazawa M, Suzuki K, Yamazaki H, Miyagawa Y. Expression profiles of cytokines and chemokines in vitreous fluid in diabetic retinopathy and central retinal vein occlusion. Jpn J Ophthalmol. 2011;55:256–63.
7. Noma H, Funatsu H, Harino S, Mimura T, Eguchi S, Hori S. Vitreous inflammatory factors in macular edema with central retinal vein occlusion. Jpn J Ophthalmol. 2011;55:248–55.
8. Koss MJ, Pfister M, Rothweiler F, Michaelis M, Cinatl J, Schubert R, et al. Comparison of cytokine levels from undiluted vitreous of untreated patients with retinal vein occlusion. Acta Ophthalmol. 2012;90:e98–103.
9. Hayreh SS, Klugman MR, Podhajsky P, Kolder HE. Electroretinography in central retinal vein occlusion. Correlation of electroretinographic changes with pupillary abnormalities. Graefes Arch Clin Exp Ophthalmol. 1989;227:549–61.
10. Hayreh SS, Klugman MR, Beri M, Kimura AE, Podhajsky P. Differentiation of ischemic from non-ischemic central retinal vein occlusion during the early acute phase. Graefes Arch Clin Exp Ophthalmol. 1990;228:201–17.
11. Breton ME, Quinn GE, Keene SS, Dahmen JC, Brucker AJ. Electroretinogram parameters at presentation as predictors of rubeosis in central retinal vein occlusion patients. Ophthalmology. 1989;96:1343–52.
12. Breton ME, Montzka DP, Brucker AJ, Quinn GE. Electroretinogram interpretation in central retinal vein occlusion. Ophthalmology. 1991;98:1937–44.
13. Breton ME, Schueller AW, Montzka DP. Electroretinogram b-wave implicit time and b/a wave ratio as a function of intensity in central retinal vein occlusion. Ophthalmology. 1991;98:1845–53.
14. Johnson MA, Marcus S, Elman MJ, McPhee TJ. Neovascularization in central retinal vein occlusion. Electroretinographic findings. Arch Ophthalmol. 1988;106:348–52.
15. Johnson MA, McPhee TJ. Electroretinographic findings in iris neovascularization due to acute central retinal vein occlusion. Arch Ophthalmol. 1993;111:806–14.
16. Severns ml, Johnson MA. Predicting outcome in central retinal vein occlusion using the flicker electroretinogram. Arch Ophthalmol. 1993;111:1123–30.
17. Kaye SB, Harding SP. Early electroretinography in unilateral central retinal vein occlusion as a predictor of rubeosis iridis. Arch Ophthalmol. 1988;106:353–6.
18. Sabates R, Hirose T, McMeel JW. Electroretinography in the prognosis and classification of central retinal vein occlusion. Arch Ophthalmol. 1983;101:232–5.
19. Matsui Y, Katsumi O, Mehta MC, Hirose T. Correction of electroretinographic and fluorescein angiographic findings in unilateral central retinal vein obstruction. Graefes Arch Clin Exp Ophthalmol. 1994;232:449–57.
20. Morrell AJ, Thompson DA, Gibson JM, Kritzinger EE, Drasdo N. Electroretinography as a prognostic indicator of neovascularization in CRVO. Eye. 1991;5:362–8.
21. Matsui Y, Katsumi O, McMeel JW, Hirose T. Prognostic value of initial electroretinogram in central retinal vein obstruction. Graefes Arch Clin Exp Ophthalmol. 1994;232:75–81.
22. Larsson J, Andreasson S, Bauer B. Cone b-wave implicit time as an early predictor of rubeosis in central retinal vein occlusion. Am J Ophthalmol. 1998;125:247–9.
23. Larsson J, Bauer B, Andreasson S. The 30-Hz flicker cone ERG for monitoring the early course of central retinal vein occlusion. Acta Ophthalmol Scand. 2000;78:187–90.
24. Larsson J, Andreasson S. Photopic 30 Hz flicker ERG as a predictor for rubeosis in central retinal vein occlusion. Br J Ophthalmol. 2001;85:683–5.
25. Kjeka O, Bredrup C, Krohn J. Photopic 30 Hz flicker electroretinography predicts ocular neovascularization in central retinal vein occlusion. Acta Ophthalmol Scand. 2007;85:640–3.
26. Kuo HK, Kuo MT, Chen YJ, Wu PC, Chen CH, Chen YH. The flicker electroretinogram interocular amplitude ratio is a strong prognostic indicator of neovascularization in patients with central retinal vein occlusion. Graefes Arch Clin Exp Ophthalmol. 2010;248:185–9.

27. Yasuda S, Kachi S, Kondo M, Ushida H, Uetani R, Terui T, et al. Significant correlation between electroretinogram parameters and ocular vascular endothelial growth factor concentration in central retinal vein occlusion eyes. Invest Ophthalmol Vis Sci. 2011;52:5737–42.
28. Noma H, Funatsu H, Mimura T. Association of electroretinographic parameters and inflammatory factors in branch retinal vein occlusion with macular oedema. Br J Ophthalmol. 2012;96:1489–93.
29. Kjeka O, Bredrup C, Krohn J. Photopic 30 Hz flicker electroretinography predicts ocular neovascularization in central retinal vein occlusion. Acta Ophthalmol Scand. 2007;85:640–3.

OPEN ACCESS Freely available online

PLOS | ONE

# Degeneration of Retinal ON Bipolar Cells Induced by Serum Including Autoantibody against TRPM1 in Mouse Model of Paraneoplastic Retinopathy

**Shinji Ueno[1*], Koji M. Nishiguchi[1], Hidetoshi Tanioka[2], Atsushi Enomoto[3], Takashi Yamanouchi[2], Mineo Kondo[1], Testuhiro R. Yasuma[1], Shunsuke Yasuda[1], Noriyuki Kuno[2], Masahide Takahashi[3], Hiroko Terasaki[1]**

1 Department of Ophthalmology, Nagoya University Graduate School of Medicine, Nagoya, Japan, 2 Research and Development Center, Santen Pharmaceutical Co., Ltd., Ikoma, Japan, 3 Department of Pathology, Nagoya University Graduate School of Medicine, Nagoya, Japan

**Abstract**

The paraneoplastic retinopathies (PRs) are a group of eye diseases characterized by a sudden and progressive dysfunction of the retina caused by an antibody against a protein in a neoplasm. Evidence has been obtained that the transient receptor potential melastatin 1 (TRPM1) protein was one of the antigens for the autoantibody against the ON bipolar cells in PR patients. However, it has not been determined how the autoantibody causes the dysfunction of the ON bipolar cells. We hypothesized that the antibody against TRPM1 in the serum of patients with PR causes a degeneration of retinal ON bipolar cells. To test this hypothesis, we injected the serum from the PR patient, previously shown to contain anti-TRPM1 antibodies by westerblot, intravitreally into mice and examined the effects on the retina. We found that the electroretinograms (ERGs) of the mice were altered acutely after the injection, and the shape of the ERGs resembled that of the patient with PR. Immunohistochemical analysis of the eyes injected with the serum showed immunoreactivity against bipolar cells only in wild-type animals and not in TRPM1 knockout mice,consistent with the serum containing anti-TRPM1 antibodies. Histology also showed that some of the bipolar cells were apoptotic by 5 hours after the injection in wild type mice, but no bipolar cell death was found in TRPM1 knockout mice, . At 3 months, the inner nuclear layer was thinner and the amplitudes of the ERGs were still reduced. These results indicate that the serum of a patient with PR contained an antibody against TRPM1 caused an acute death of retinal ON bipolar cells of mice.

**Citation:** Ueno S, Nishiguchi KM, Tanioka H, Enomoto A, Yamanouchi T, et al. (2013) Degeneration of Retinal ON Bipolar Cells Induced by Serum Including Autoantibody against TRPM1 in Mouse Model of Paraneoplastic Retinopathy. PLoS ONE 8(11): e81507. doi:10.1371/journal.pone.0081507

**Editor:** Erica Lucy Fletcher, The University of Melbourne, Australia

**Received** April 7, 2013; **Accepted** October 14, 2013; **Published** November 25, 2013



**Funding:** Grant-in-Aid for Scientific Research (B)(#23791977) from the Ministry of Education, Culture, Sports, Science and Technology(http://www.jsps.go.jp/). The funders had no role in study design, data collection and analysis, decision to publish, or preparation of the manuscript.

**Competing interests:** H. Tanoika, TY & NK are employees of Santen Pharmaceutical Co., Ltd. There are no patents, products in development or marketed products to declare. This does not alter the authors' adherence to all the PLOS ONE policies on sharing data and materials.

* E-mail: ueno@med.nagoya-u.ac.jp

## Introduction

Light stimulation of the rod and cone photoreceptors elicits signals that are transmitted to the bipolar cells and then to the retinal ganglion cells (RGCs). At present, there are many retinal diseases that are caused by a degeneration of the photoreceptors or the RGCs. Retinitis pigmentosa is an example of the former type of diseases and is caused by a degeneration of the rods followed by the cones. Glaucoma is an example of the second type of diseases that is caused by the death of RGCs. There is no known retinal disease caused by bipolar cell degeneration.

The paraneoplastic retinopathies (PRs) are a group of diseases characterized by a sudden and progressive decrease in the function of the retina. The retinopathies have been shown to be caused by a circulating anti-retinal autoimmune antibody against a protein of a neoplasm [1-4]. One subtype of the PRs has been reported to be caused by an autoantibody against a protein expressed by retinal ON bipolar cells [5,6]. The symptoms and signs of these patients were a sudden onset night blindness, photophobia, and a decrease of the visual acuity. The electroretinograms (ERGs) elicited by a standard flash stimuli had a selective reduction of the b-waves with normal a-waves. This resulted in a waveform called a negative type ERG which suggested a dysfunction of the ON bipolar cells. Additional ocular examinations including fundus examination showed no distinctive features [6]. Originally these diseases were reported in patients with melanomas, and they

were named melanoma-associated retinopathies (MARs) [7,8]. However, it has been reported that neoplasms other than melanomas can cause the bipolar cell dysfunction [5,9].

We and others have recently shown that the transient receptor potential melastatin 1 (TRPM1) was an antigen for the autoantibody against the ON bipolar cells in some patients with PR [10,11]. TRPM1 is a protein associated with the ion-conducting plasma membrane channels that mediates the light responses of ON bipolar cells [12-14]. Several studies have reported the presence of neural degeneration in the paraneoplastic syndrome including other types of paraneoplatic retinopathies [4,15-17], but none have shown that the serum of patients with PR can cause a degeneration of the retinal ON bipolar cells.

Thus, the purpose of this study was to determine whether the serum of a PR patient with the TRPM1 antibody will cause a degeneration of ON bipolar cells. To achieve this, we injected serum from a PR patient who had an autoantibody against TRPM1 [11] into the vitreous of mice and evaluated its effects on retinal function and histology. We show serum including autoantibody against TRPM1 caused acute retinal ON bipolar cell degeneration.

## Materials and Methods

### Animals

All experimental procedures adhered to the ARVO Statement for the Use of Animals in Ophthalmic and Vision Research and the guidelines for the Use of Animals at the Nagoya University School of Medicine. Nagoya University Animal Experiment Committee approved this project (approval number 24456). Seventy C57BL/6 mice at 7-10 weeks-old-age were used. TRPM1 knock-out mice were kindly given to us by Dr. T. Furukawa of Osaka Bioscience Institute [14].

### Human

The Nagoya University Hospital Ethics Review Board approved this study (approval ID 1131). The procedures used conformed to the tenets of the Declaration of Helsinki of the World Medical Association. A written informed consent was obtained from the patient after he was provided with sufficient information on the procedures to be used.

### Sera and intravitreal injections

Sera were collected from one PR patient and one visually normal male subject. The patient had lung cancer and the negative type ERG, and his eye phenotype has been described in detail [11]. Mice were anesthetized with ether, and 1 µL of the serum of the patient or control subject was injected intravitreally into C57BL/6 mice. Other C57BL/6 mice had l-2 amino-4-phosphonobutyric acid (APB; Sigma-Aldrich, St. Louis, MO) solution injected into the vitreous. The APB was dissolved in sterile saline, and the intravitreal concentration was estimated to be 1 mM. The injections were made with a glass micropipette with a microinjection apparatus (IM 300 microinjection; Narishige, Tokyo, Japan).

### Electroretinograms (ERGs) of mice

To evaluate the function of the retina after the intravitreal injection of the sera and APB, five C57BL6 mice were injected with the PR patient's whole serum in one eye and the serum of the control subject in the other eye. ERGs were recorded at 3 hrs, 3 days, 1 month, 3 months, and 6 months after the injection. We also recorded ERGs from 6 mouse eyes 3 hours after the intravitreal injection of APB solution to determine the effect of blocking the ON bipolar cell on the ERGs [18]. The procedures used for the ERG recordings have been described in detail [19]. Scotopic ERGs were elicited by stimulus intensities of -2.6 and 1.0 log cd-s/$m^2$ after one hour of dark-adaptation, and the photopic ERGs were elicited by a stimulus intensity of 1.0 log cd-s/$m^2$ presented on a rod saturating background of 40 cd/$m^2$.

### Western blot analyses

The cDNAs for human and mouse TRPM1 were generously provided by Dr. T. Furukawa of the Osaka Bioscience Institute, and Western blots were performed as described [11]. HEK293FT cells (Invitrogen, Carlsbad, CA) were grown and transfected with control plasmids (Flag-GST), mouse TRPM1 (mTRPM1), or human TRPM1 fused to the 3xFlag epitope at the carboxyl terminus (hTRPM1-Flag). The antibodies used included anti-mouse TRPM1 (1:100), anti-Flag (1:1000; Sigma, St Louis, MO), and anti-β-actin (1:5000; Sigma).

### Immunohistochemical analyses

Eyecups from mice were fixed in 4% paraformaldehyde in phosphate-buffered saline (PBS) for 1 hour and placed in 30% sucrose in PBS overnight at 4° C. The eyecups were embedded in OCT compound (Tissue-Tek; Sakura Finetek Japan Co. Ltd., Tokyo, Japan), and 12-18 µm thick frozen sections were cut along the radial axis of the eye. After the sections were permeabilized in 0.1% Triton X-100 in PBS for 15 minutes, they were blocked in 4% goat serum in PBS for 30 minutes. They were then incubated with primary antibodies for 1 hour and for another hour in a mixture of secondary antibodies and diamino-2-phenyl-indol (DAPI; Molecular Probes, Life Technologies, Carlsbad, CA). The primary antibody was omitted for the immunostaining of anti-human IgG. Rabbit anti-protein kinase C α subunit (PKCα) (1:500 Sigma-Aldrich; St Louis,MO) and rat anti-F4/80 (1:400; AbD Serotec, Oxford,UK) were used as the primary antibodies. Goat anti-human-IgG-Alexa488, goat anti-rabbit-IgG-Alexa488, and goat anti-rat-IgG-Alexa488 (Molecular Probes; Life Technologies; Carlsbad, CA) were used as the secondary antibodies and were diluted by 1:500 in PBS.

### TdT-mediated dUTP-biotin nick-end labeling (TUNEL) staining

To detect apoptotic cells, the sections were stained with an *in situ* apoptotic cell detection kit (Click it TUNEL Alexa Fluor 488, Invitrogen). TUNEL staining was performed on retinal sections obtained 1 day after the serum injection. The number of TUNEL-positive cells in the INL was counted in three independent images (180 x 240 µm) from one eye and

averaged. Three eyes that were injected with the control serum and three eyes injected with the patient's serum were examined. The number of DAPI-positive nuclei in the INL was also counted.

### Transmission Electron Microscopic (TEM) Examinations

Three eyes from 3 mice injected intravitreally with the serum from the control subject and three eyes with the serum from the patient with PR were enucleated after 5 hours, 3 days, and 3 months. The eyes of two TRPM1 knockout mice of 9-weeks-of-age were obtained at 5 hours after the injection of the patient's serum. All of the eyes were fixed in 2.5% glutaraldehyde in 0.1 M PBS, washed 3 times in PBS, and postfixed for 1 hour in 1% aqueous osmium tetroxide. They were then dehydrated in a graded ethanol series, transferred to QY-1 (Nissin EM, Tokyo, Japan), and embedded in Quetol-812 (Nissin EM, Tokyo, Japan). Semi-thin sections were cut and stained with 0.05% toluidine blue for light microscopy (LM). Ultrathin sections were stained with uranyl acetate and lead citrate and examined with a TEM (H-7600; Hitachi, Tokyo, Japan).

### Hematoxylin-eosin (HE) staining

Three months after the intravitreal injection of the serum from the control subject into 6 eyes and serum from the PR patient into 6 eyes of C57BL6 mice, the eyes were enucleated and fixed overnight in a mixture of 10% neutral buffered formalin and 2.5% glutaraldehyde. The eyes were transferred to 10% formalin. The tissues were embedded in paraffin, sectioned vertically through the optic nerve so that the superior and inferior halves could be examined. The mounted sections were stained with hematoxylin and eosin (HE). The thickness of the combined inner nuclear layer (INL) and outer plexiform layer (OPL) and outer nuclear layer (ONL) were measured every 400 μm across both the superior (S1-3) and inferior hemispheres (I1-3). We calculated the ratio of the thickness of the INL +OPL/ONL to reduce any artifacts produced during the processing of the tissues.

### Photography

HE and toluidine blue stained sections were photographed with a Nikon Eclipse TE 2000 microscope or with a Digital sight DS-U1. For the immunohistochemical analyses and TUNEL assays, photographs were taken with a confocal D-Eclipse C1 microscope (Nikon, Tokyo,Japan). Photomicrographs were from the retina near the post pole, and images of immunohistochemical analysis of PKCα were taken from the peripheral to mid peripheral retina.

### Statistical analyses

Student's *t* tests were used to determine the significance of any differences in the thickness of the retinal layers and evaluation of the ERG amplitudes. A $P < 0.05$ was considered significant.

## Results

### Reduction of scotopic b-wave and relative preservation of a-wave in ERG induced by itravitreal injection of patient's serum in mice

Representative Ergs recorded from eyes 3 days after the intravitreal injection of the serum from a control subject and the serum from the PR patient are shown in Figure 1A. Also shown are the ERGs recorded 3 hours after the intravitreal injection of APB. The ERGs of the eye that received the control serum has a positive b-wave of about 200 μV that was elicited by a dim flash under scotopic conditions(-2.6 log cd-s/m$^2$). With a bright flash of 1.0 log cd-s/m$^2$, the ERG consisted of a negative a-wave of about 300 μV and a b-wave of about 600 μV under scotopic conditions. Under photopic conditions, the ERG consisted of a small a-wave and a b-wave of about 200 μV. In contrast, the ERGs of the eye that received the patient's serum elicited by a scotopic dim flash was almost extinguished. With a bright flash, the a-wave amplitude was similar to that of the control but the b-wave was markedly reduced. This resulted in a negative type ERG (a-wave>b-wave). The b-wave amplitudes of the photopic ERGs were also reduced. The ERGs after APB injection had almost the same pattern of ERGs recorded after the patient serum injection.

The ERGs recorded from the PR patient and from a control subject are shown in Figure 1B. These ERGs were recorded under approximately the same conditions as the ERGs in the mice. The ERGs of the patient resembled very closely the ERGs of the mouse that had received the patient's serum; almost non-recordable b-wave with a dim flash and a negative waveform ERG with a bright flash under scotopic conditions. Under photopic conditions, the ERG of the patient had large wide a-wave and small and delayed b-wave. Although the waveform resembled that of non-human primates intravitreally injected with APB to block the function of ON bipolar cells, the result seemed to oppose to that of the mouse ERGs that were markedly reduced (see discussion) [20,21].

The a-wave was measured from the baseline to the first negative trough and the b-wave was measured from the bottom of the a-wave to the peak of the following positive wave (Figure 1C).□We followed the ERGs of 5 mice for up to 6 months after the injection of the patient's serum in one eye and the control serum in the other eye. We measured the amplitudes of the a- and b-waves elicited by the scotopic bright flashes (1.0 log cd-s/m$^2$). Because the a-waves originate from photoreceptor activity [22-24], they were used to assess the function of the photoreceptors. In the same way, the b-waves originate from ON bipolar cells, and they were assessed to estimate the function of the ON bipolar cells [25]. We also used the b-/a-wave amplitude ratio of the scotopic bright flash ERGs to assess the functioning of the postsynaptic neurons. A low b-/a-wave ratio would indicate reduced postsynaptic activity relative to that of the photoreceptors.

The mean amplitude of a-wave of the two types of eyes was not significantly different at all time points. However, the amplitude of the b-wave and b-/a-wave ratios were reduced after 3 hours and did not recover for at least 6 months after the injection (Figure 1D). These results indicated that the function

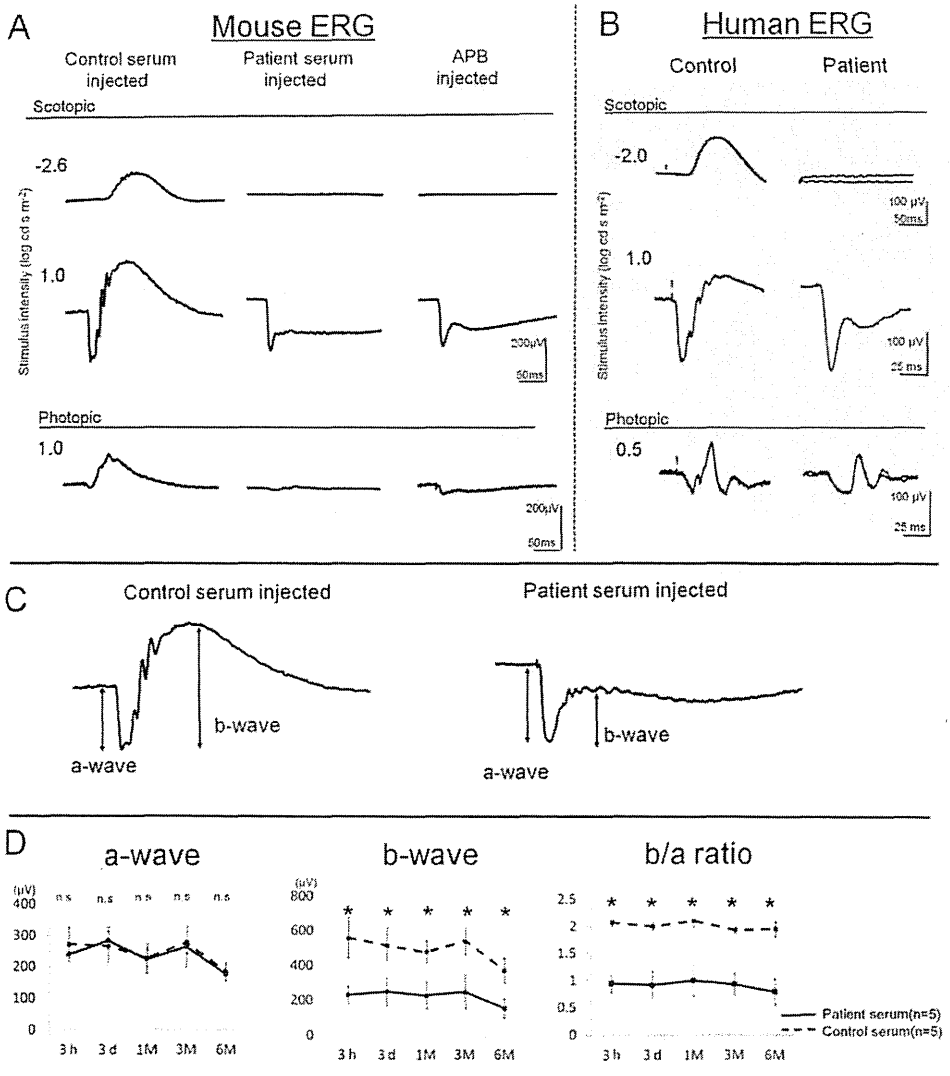


**Figure 1. Electroretinograms (ERGs) recorded after an intravitreal injection of serum.** (A) Representative Ergs of mice that received an intravitreal injection of serum from a normal control subject, the serum of a PR patient and APB solution.
(B) For comparison, ERGs of a control subject and the patient are shown. ERGs were elicited under 3 conditions; scotopic dim flash, scotopic bright flash, and photopic bright flash.
(C) Representative Ergs recorded 3 days after the injection of the control and patient sera into the vitreous. The ERGs were elicited by 1.0 log cds $m^{-2}$ for the scotopic condition. The a-wave was measured from baseline to first negative trough, and the b-wave was measured from the bottom of a-wave to the peak of the following positive wave as indicated by the arrows.
(D) Amplitudes of a-wave, b-wave, and b/a ratio recorded at 3 hours, 3 days, 1 month, 3 months, and 6 months after the serum injection are plotted (mean ± SEM ,n=5; *$P$<0.05 ).
doi: 10.1371/journal.pone.0081507.g001

of the ON bipolar cells was depressed within 3 hours after the injection of the patient's serum, and the reduction persisted for at least 6 months.

### Autoantibody against TRPM1 in patient's serum

To confirm that the injected IgG in the patient serum was against TRPM1, we immunostained the retinas obtained 5 hours after the intravitreal injection of the serum with anti-human IgG, a secondary antibody. The immunohistochemical findings of the retina from a mouse that received the control

**Figure 2. Immunostaining with anti-human IgG antibody of mouse retina obtain 5 hours after intravitreal injection of serum.** Immunostaining of mouse retina that was injected with control serum (A), with the patient's serum (B), and immunostaining of TRPM1 knockout mouse retina with the patient's serum (C). Human IgG was stained green. The regions indicated by the white boxes are enlarged below and stained with DAPI in blue (bottom of A, B and C). Fluorescein staining is prominent in the OPL (B). The scale bar is 25 μm in panels (A) to (C).

(D) Immunoblots of transfected cell lysates using an antibody against Flag tag, antibody against mouse TRPM1, serum from PR patient, and serum from control subject. Arrowheads indicate the TRPM1-Flag protein bands and arrow indicates mouse TRPM1 protein. β-actin (β-act) was used for loading control. Patient serum had autoantibodies against both mouse and human TRPM1. Abbreviations: ILM - inner limiting membrane, RGC - retinal ganglion cells, IPL-inner plexiform layer, INL - inner nuclear layer, OPL - outer plexiform layer, ONL - outer nuclear layer.

doi: 10.1371/journal.pone.0081507.g002

serum, the retina of a mouse that received the patient's serum, and the retina of a TRPM1 knockout mouse that received the patient's serum are shown in Figures 2A-2C. In the TRPM1 knockout mouse, no reduction of the retinal ON bipolar cell markers including Chx10, Goα, and mGluR6 except TRPM1 was observed and the retinal morphology appeared to be normal [14]. Because some of the IgG in the injected serum was retained in the vitreous and inner limiting membrane (ILM), the ILM were stained in the three types of mice (Figures 2A-2C). Punctate staining was present in the OPL in the mouse after the injection of the patient's serum (Figures 2B), but only weak uniform background staining was detected in the other two retinas (Figures 2A and 2C). The distribution of these punctate staining agreed with the report of immunostaining of TRPM1 on the dendritic tips of the retinal ON bipolar cells [14]. The absence of staining in the TRPM1 knock out mouse strongly suggested that the antibody was against TRPM1 or a protein whose expression was dependent on TRPM1.

We also performed Western blots to confirm that the patient's serum would recognize both human and mouse TRPM1. We transfected HEK293FT cells with expression plasmids containing control, human TRPM1-Flag (hTRPM1-Flag), or mouse TRPM1 (mTRPM1). Western blot analysis was performed on whole cell extracts, and we confirmed that a hTRPM1-Flag band and a mTRPM1 band were present at about 200 kDa in the cell lysates (Figure 2D). Next, we performed Western blot analysis on the same lysates using the serum from our patient and a control subject. We detected

immunostaining of the same size proteins in both TRPM1-Flag and mTRPM1 with the patient's serum (Figure 2D; Patient serum). The blots with the control serum did not have a significant band. These results showed that the autoantibody was reactive to both human and mouse TRPM1.

### Acute cell death in INL caused by injection of patient serum

Photomicrographs of the retinas of mice injected with the control serum, the patient's serum, and a retina from a TRPM1 knockout mouse injected with the patient's serum are shown in Figure 3. Retinal sections of eyes obtained 5 hours after the injection of the patient's serum were examined by light microscopy (LM; Figure 3A-3C) and transmission electron microscopy (TEM; Figure 3D-3I). The toluidine blue stained retina of the mouse injected with the patient's serum had many densely stained nuclei in the inner nuclear layer (INL) especially on the photoreceptor side (Figure 3B, arrows). We also examined the INL for any abnormalities by TEM. Low magnification TEM showed densely stained nuclei located on the photoreceptor side of the INL (Figure 3B). High magnification TEM showed nuclear fragmentation and chromatin condensation in these nuclei (Figure 3H; asterisk). LM and TEM showed no obvious abnormalities in the INL of the retina of the two other types of retinas (Figure 3A, 3C, 3D, 3F, 3G, and 3I).

TUNEL staining was performed on retinas obtained 1 day after the serum injection (Figure 3J-3L). TUNEL-positive cells were detected in the INL where both toluidine blue stain and TEM showed abnormally stained nuclei (Figure 3 K). The number of TUNEL-positive cells/INL cells was 15.5 ± 8.0/162.7 ± 16.5 (mean ± SD) in the retina injected with the patient's serum. In contrast, the retina of two other groups did not have any TUNEL-positive cells in the INL (Figure 3J and 3L). Thus, the absence of TUNEL-positive cells in the TRPM1 knockout mice supported the conclusion that the autoantibody against TRPM1 was implicated in cell death.

### Loss of bipolar histochemical and structural markers after injection of patient serum

To determine the distribution of ON bipolar cells, we performed immunohistochemical analysis using antibody against protein kinase C alpha subunit (PKCα) which is a marker of rod ON bipolar cells [26]. PKCα is located in the cell bodies, the dendrites, and the synaptic terminals of rod ON bipolar cells [27,28]. High magnification photomicrographs showed that the PKC α-positive cell bodies were located mainly on the photoreceptor side of the INL where the condensation of nuclei was found (Figure 3B). PKCα staining was present in the retina at 5 hours after the patient's serum injection and at 24 hours after control serum injection (Figure 4A and 4B, arrows). However, PKCα staining was absent in most of the retina excluding the periphery at 24 hours after the injection of patient serum, (Figure 4C, arrows). These results supported the conclusion that PKCα was down-regulated or the ON bipolar cells had degenerated. Conversely, PKCα staining was found in TRPM1 KO mouse even at 24 hours after the injection of the patient's serum (Figure 4D, asterisk). These results indicated that PKCα staining was absent because of the interaction between the patient's sera and TRPM1 protein. We evaluated 3 retinas from each time point and obtained the same results.

We then examined the ultrastructure of the OPL and especially the synapses between the photoreceptors and ON bipolar cells. Dendrites of the retinal ON bipolar cells reached the ribbon synapses of photoreceptors. We focused on the abnormalities of the dendrites of retinal rod ON bipolar cells. Photomicrographs of the OPL of a mouse 5 hours after the injection of the control serum or patient's serum are shown in Figures 5A and 5B, respectively. In the retina of the mouse that received the control serum, the photoreceptor synaptic ribbons were surrounded by the dendrites of two horizontal cells and that of one invaginated rod ON bipolar cell (Figure 5A insertion) [29]. In the retina that received the patient's serum, the invaginated rod ON bipolar cell dendritic terminal that extend to the ribbon synapse was darkly stained (Figure 5B, arrowhead). The structures in the retinal rod ON bipolar cells were darkly stained but horizontal cell were not affected (Figure 5B insertion). These observations suggested a degeneration of dendrites [30,31]. Other parts of the retina, the retinal pigment epithelium (RPE), photoreceptor outer and inner segments, ONL, and RGCs, appeared not to be affected by the patient's serum (Figure 5C-5E).

### Macrophages in INL three days after patient serum injection

Toluidine blue stained retinal sections obtained 3 days after the injection of control serum and patient's serum are shown in Figures 6A and 6B, respectively. Nuclear condensation was observed 5 hours after the patient serum injection (Figure 3 B) but none was present 3 days after the injection (Figure 6B). When the INL was examined by TEM, macrophages were found surrounding the apoptotic cells (Figure 6C). F4/80-positive macrophages were detected (Figure 6E) in the layer in which TUNEL-positive cells were detected in Figure 3K. But the number of F4/80-positive cells was low, and we were able to detect only 1 to 2 cells/field (180 x 240 μm) in the immunohistochemical examinations. These results suggested that macrophages and/or other phagocytic cells had probably cleared the apoptotic cells detected in Figure 3B.

### Progressive loss of bipolar cells detected 3 months after patient serum injection

The HE stained retinas obtained 3 months after the patient's serum had neither nuclear condensation which was observed 5 hours after injection in INL nor distortion of retinal layers including ONL, INL and RGC compared to the retina after control serum injection (Figure 7A). We suggest that this was because of the phagocytosis of the apoptotic cells in the INL (Figure 6). To confirm this, we measured the thickness of INL and the OPL of the two groups of mice; the INL is where the ON bipolar cell bodies are located and the OPL where the dendrites are located. Because the OPL was too thin to measure, we evaluated the INL+OPL. We also measured the thickness of the ONL as shown in Figure 7A. The location 400μm , 800μm and 1200 superior to the optic disc were defined as S-3,S-2, and S-1 respectively, and the location

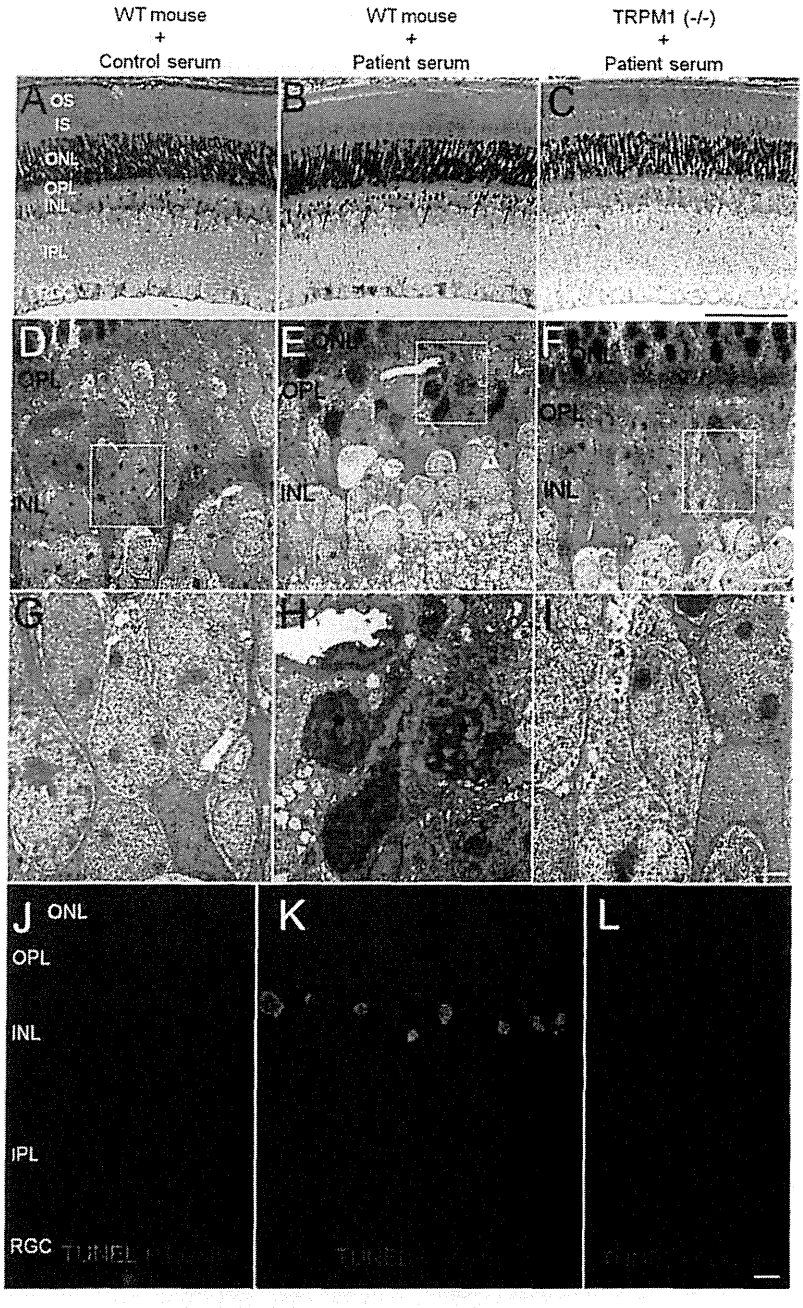


**Figure 3. Light microscope (LM) and transmission electron microscope (TEM) photomicrographs of retinal sections.** (A-C) LM photomicrographs of toluidine blue stained section obtained 5 hours after an intravitreal serum injection. (D - I) TEM photomicrographs of retinas at the same time point. (J - L) TUNEL (green) with Hoechst staining of retina obtained 1 day after the serum injection. Photomicrographs of retina from wild mouse that had the control serum injection (A, D, G, and J), the PR patient's serum injection (B, E, H, and K) and retina from TRPM1 knockout mouse that had the patient's serum injection. (C, F, I, and L). Photomicrographs of the regions outlined by the white boxes (D, E, and F) are enlarged below in (G, H, and I) respectively. Wild mouse retina after the injection of the patient's serum shows many densely stained nuclei in the INL (B, arrow), and high magnification of TEM shows nuclear fragmentation and chromatin condensation of these cells (H, asterisk). Many TUNEL positive cells can be seen in the INL (K). The scale bar in the left row applies to the other two rows. The scale bar; C = 100 μm, F = 10 μm, I= 2 μm, and L = 10 μm.

doi: 10.1371/journal.pone.0081507.g003